Optical Engineering

SPIEDigitalLibrary.org/oe

Microcavity strain sensor for high temperature applications

Amardeep Kaur
Steve E. Watkins
Jie Huang
Lei Yuan
Hai Xiao

SPIE

Microcavity strain sensor for high temperature applications

Amardeep Kaur,[a] Steve E. Watkins,[b,*] Jie Huang,[a] Lei Yuan,[a,c] and Hai Xiao[a]
[a]Missouri University of Science and Technology, Photonics Technology Laboratory, Department of Electrical and Computer Engineering, 1870 Miner Circle, Rolla, Missouri 65409-0040
[b]Missouri University of Science and Technology, Applied Optics Laboratory, Department of Electrical and Computer Engineering, 1870 Miner Circle, Rolla, Missouri 65409-0040
[c]Beijing Institute of Technology, Laser Micro/Nano Fabrication Laboratory, School of Mechanical Engineering, Beijing 100081, China

Abstract. A microcavity extrinsic Fabry–Perot interferometric (EFPI) fiber-optic sensor is presented for measurement of strain. The EFPI sensor is fabricated by micromachining a cavity on the tip of a standard single-mode fiber with a femtosecond (fs) laser and is then self-enclosed by fusion splicing another piece of single-mode fiber. The fs-laser-based fabrication makes the sensor thermally stable to sustain temperatures as high as 800°C. The sensor exhibits linear performance for a range up to 3700 $\mu\varepsilon$ and a low temperature sensitivity of only 0.59 pm/°C through 800°C. [DOI: 10.1117/1.OE.53.1.017105]

Keywords: optical fiber sensor; extrinsic Fabry–Perot interferometric; femtosecond-laser; micromachining; temperature; strain analysis.

Paper 131490P received Sep. 30, 2013; revised manuscript received Dec. 26, 2013; accepted for publication Dec. 30, 2013; published online Jan. 24, 2014.

1 Introduction

Optical fiber-based sensors have gained wide application for strain monitoring due to their compact size, immunity from electromagnetic interference, multiplexing capabilities etc. thus offering an alternative to traditional electrical sensors and conventional pneumatic-based sensors.[1–3] Different types of optical fiber instruments like fiber Bragg grating sensors, extrinsic Fabry–Perot interferometric (EFPI) sensors, intrinsic Fabry–Perot interferometric (IFPI) sensors, long-period fiber grating sensors, and related hybrid combination sensors have been used for monitoring strain, stress, temperature, and pressure.[3–7] Temperature sensitivity and temperature maximums are important practical limitations for many of these sensors. For instance, the temperature sensitivity of Bragg grating and IFPI sensors are well known.[8,9]

The EFPI-type sensors are better suited for strain monitoring applications with high ambient temperatures as opposed to Bragg gratings and IFPI sensors. These rugged sensors have excellent noise-free performance and fatigue characteristics.[10] The most widely used method for realizing the EFPI sensor is by epoxying two pieces of fiber, with cleaved ends, inside a hollow tube (glass or ceramic) and controlling the separation distance between the two fiber-ends.[11–15] In addition to the cumbersome fabrication process and the calibration issues related to controlling the cavity gap, this design has limited thermal performance due to the thermal expansion of the tube and the temperature limitation of the epoxy, e.g., Loctite epoxy extra time pro (slow setting) is effective up to 150°C once cured. Alternative approaches with low temperature sensitivities have been demonstrated by splicing a hollow-core fiber between two sections of single-mode fiber,[16] by forming voids at splices between photonic crystal fiber and conventional single-mode fiber,[17–19] and by laser-machining micro-cavities into single-mode fiber.[20] The microcavity sensor in Ref. 20 provides easily reproducible characteristics, but it has an open cavity design that exposes the cavity to the environment. In particular, this open cavity limits embedded applications. An EFPI sensor can also be fabricated using wet chemical etching in which diluted hydrofluoric acid forms a cavity in the tip of a multimode fiber, and this cavity is fused with a single-mode fiber.[21] This latter EFPI alternative has good temperature characteristics, but it suffers from safety concerns during fabrication and from difficulty in controlling the etch, i.e., for calibrating the cavity length.

In this work, a microcavity EFPI strain sensor is fabricated using femtosecond (fs) laser micromachining to form the cavity and is self-enclosed with a fusion splice. This sensor is less bulky than a tube-based EFPI, the fs-laser processing is fast and the resulting cavity length is precisely controlled, and the performance is relatively temperature insensitive and is thermally stable. The sensor is capable of operating in high-temperature applications. Fabrication, strain performance, and thermal effects are discussed.

2 Microcavity Sensor Design and Fabrication

The overall optical response for a Fabry–Perot cavity depends on multiple-beam interference in light transmitted and reflected from the two ends of the cavity. This periodic response is modulated by the wavelength and optical path (gap) length.[22] Figure 1(a) shows a traditional EFPI design in which the cavity is formed between the end faces of optical fiber that are aligned with an epoxied capillary tube.[11–14] In a strain sensor with an air gap of length d, the gauge length, i.e., the length of the sensing element, is approximately the tube length L and the measured strain is $\Delta L/L = \Delta d/L$. Figure 1(b) shows the microcavity EFPI

*Address all correspondence to: Steve E. Watkins, E-mail: steve.e.watkins@ieee.org

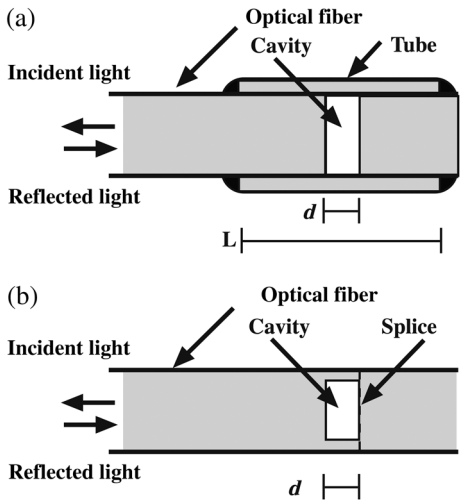

Fig. 1 (a) Traditional tube-based extrinsic Fabry–Perot interferometric (EFPI) sensor and (b) microcavity EFPI sensor.

in which the cavity is formed in the fiber itself and a second fiber is fusion spliced to self-enclose the cavity. As a strain sensor with an air gap of length d, the gauge length is the cavity gap length d and the measured strain is $\Delta d/d$. The smaller gauge length allows the latter sensor to more closely approximate a point sensor. Also, the tube component causes the former design to be bulkier and to have a more complex fabrication than the microcavity design. Note that the exact gauge length and the initial gap length are more difficult to determine for the traditional design, hence calibration is an issue.

The EFPI response is dependent on any parameter changing the cavity optical path length. For the bare sensor with no applied strain, e.g., a sensor not attached to a structure to be measured, changes in ambient temperature T induces a Δd due to the thermal expansion of the silica fiber. Since the coefficient of thermal expansion (CTE) for silica ($0.55 \times 10^{-6}/°C$) is small, this temperature dependence is minimal. Hence, the single-mode silica fiber EFPI is an ideal candidate for high-temperature applications. The smaller gauge length and the absence of epoxy reduce the influence of temperature on the microcavity EFPI performance.

The microcavity EFPI has two glass-air interfaces with low reflectivity, which produces a sensor with low finesse F. The reflectance (ratio of the output signal irradiance I_R to the input signal irradiance I_i) is[22]

$$I_R/I_i = F\sin^2(2\pi d/\lambda)/[1 + F\sin^2(2\pi d/\lambda)], \quad (1)$$

where $n = 1$ is the refractive index of the cavity and λ is the wavelength. The condition for destructive interference is

$$4\pi d/\lambda = (2\ m + 1)\pi, \quad (2)$$

where m is an integer. Note that d can be calculated from adjacent minima at λ_1 and λ_2 as

$$4\pi d/\lambda_2 - 4\pi d/\lambda_1 = (2\ m + 1)\pi - [2(m + 1) + 1]\pi \quad \text{or}$$
$$d = (1/2)\lambda_1\lambda_2/(\lambda_2 - \lambda_1). \quad (3)$$

Demodulation methods for the microcavity EFPI are the same as for the traditional EFPI types. For this work, the phase tracking method is used, cf. Ref. 15, and wavelength shifts in the interference spectrum were measured. By Eq. (2), a change in cavity length Δd is proportional to the associated wavelength change for destructive interference $\Delta\lambda$. Hence, the measured strain is

$$\Delta d/d = \Delta\lambda/\lambda. \quad (4)$$

Figure 2 shows the micromachining system with a fs laser. The single-mode fiber is cleaved and the fiber tip is aligned with a five-axis translation stage (resolution 1 μm). The fs laser is focused on the fiber tip and a cavity is precisely ablated as shown in Fig. 3. The fs-laser system (maximum output of 1 W) operates at a center wavelength of 800 nm with the repetition rate and pulse width of 250 kHz and 200 fs, respectively. The laser power used for fabrication was 0.4 μJ per pulse. The sensor fabrication is completed by fusion splicing another single-mode fiber. The resulting cavity is $65 \times 65 \times 35\ \mu m^3$ (see Fig. 3).

3 EFPI Sensor Testing

Figure 4(a) shows the instrumentation used for sensor testing. A 100-nm broadband source is the input, a 3-dB coupler sends the signal to the sensor and receives the reflected signal back, and an optical spectrum analyzer (OSA) then records the wavelength spectra. Figure 4(b) shows the spectra shift for an applied 500-$\mu\varepsilon$ strain. Several microcavity EFPI sensors were fabricated with similar cavity lengths (~35 μm),

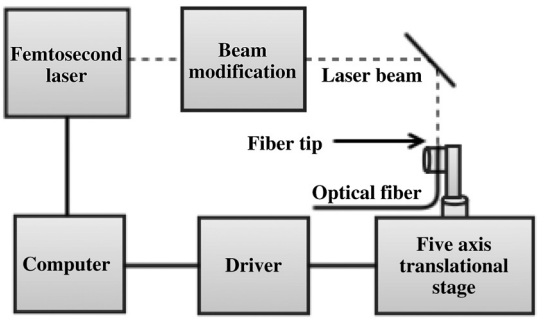

Fig. 2 Femtosecond-laser micromachining system.

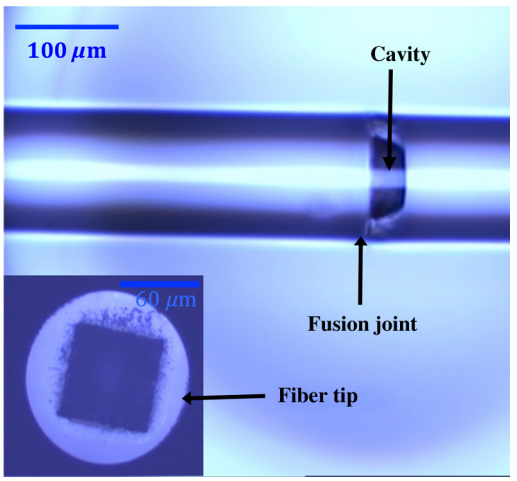

Fig. 3 Confocal microscopic image of the microcavity (side view and tip view).

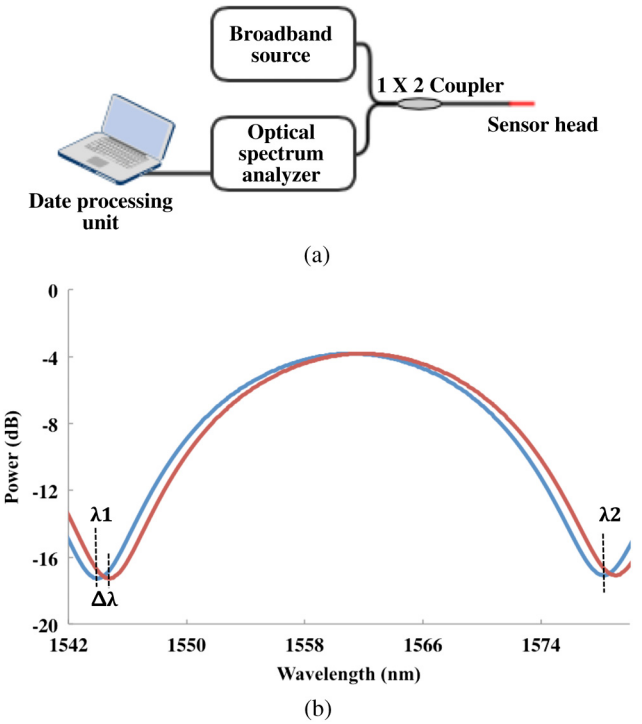

Fig. 4 (a) Instrumentation for EFPI sensor testing and (b) wavelength spectra shift for an applied 500-$\mu\varepsilon$ strain.

fringe visibility (10 to 12 dB), and excess loss (4 to 6 dB) (The excess loss is the nonideal power drop, e.g., for destructive interference the return signal is −4 to −6 dB down from the ideal value of 0 dB.).

Figure 5 shows the strain-induced response of the microcavity sensor at room temperature. The wavelength spectra shift is plotted with respect to the applied strain. The sensor was fixed between two translational stages and axial strain was applied in steps of 100 $\mu\varepsilon$. The sensor response was linear with response slope of 1.5 pm/$\mu\varepsilon$. The strain was applied until the sensor broke at the fusion joint as verified under a microscope. The breaking point for the EFPI sensor was 3700 $\mu\varepsilon$ approximately. The figure inset shows detailed performance for strains applied from 1000 through 1500 $\mu\varepsilon$.

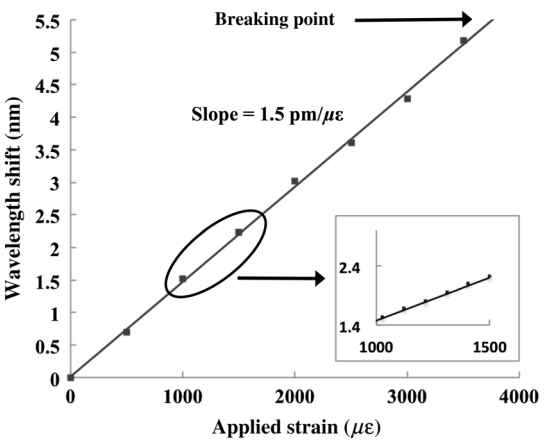

Fig. 5 Wavelength spectra shift for applied strain at room temperature.

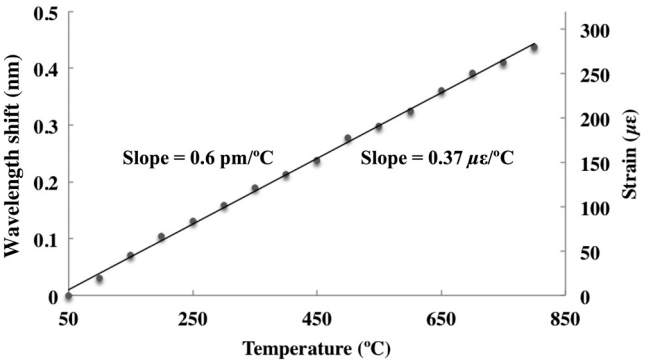

Fig. 6 Temperature dependence of the wavelength spectra shift and the apparent strain.

Figure 6 shows the temperature-induced wavelength shift with no applied strain. For the temperature testing, the sensor was placed inside a box furnace (Lindberg/Blue M). The temperature of the furnace was raised from 50°C to 800°C in steps of 50°C, and the resultant wavelength shift in the spectrum was recorded using the OSA. The results are plotted in terms of wavelength shift as well as the apparent strain. The slopes of the experimental response for the EFPI sensor were 0.59 pm/°C and 0.37 $\mu\varepsilon$/°C for wavelength shift and apparent strain, respectively. The CTE of silica was calculated to be

$$\mathrm{CTE} = (\Delta d/d)/\Delta T = 0.715 \times 10^{-6}/^{\circ}\mathrm{C}$$

that is 1.3 times larger than that of the reference silica CTE of $0.55 \times 10^{-6}/^{\circ}\mathrm{C}$.

The design's capability for handling high temperatures was also tested by keeping a second identical sensor at 650°C for 3 h. No change in the reflection spectrum was observed during this 3-h test. The sensor was then returned to room temperature and temperature-induced wavelength shift with no applied strain was again determined. The sensor survived the whole process without any deterioration in the performance, i.e., it had the same responses as given in Fig. 6 for the sensor with no prior high temperature history.

4 Conclusions

A robust, compact EFPI strain sensor is demonstrated that is easy to fabricate and calibrate and that has a high operating temperature. A single fusion joint allows for better structural integrity and is less complicated compared to traditional designs. The fs-laser fabrication results in well-controlled cavity for calibration. The wavelength shift with applied strain is linear up to a breaking point of about 3700 $\mu\varepsilon$. The sensor has a low cross sensitivity due to low thermal expansion of the silica glass, i.e., the wavelength shift with temperature is small up to at least 800°C. The experimental CTE value was slightly higher than the reference value for silica. Ongoing work is examining the sensor performance for embedded applications in which the sensor must survive high-temperature fabrication processes and must monitor strain at elevated temperatures. Preliminary results show successful sensor operation and strain transfer while embedded in carbon fiber composite laminate plate.[23] Overall, the microcavity EFPI is a good candidate for strain monitoring applications in high ambient temperatures.

Acknowledgments

The authors acknowledge the support of National Science Foundation project under grant CMMI-1200787.

References

1. E. Udd, "An overview of fiber-optic sensors," *Rev. Sci. Instrum.* **66**(8), 4015–4030 (1995).
2. R. Kashyap, "Photosensitive optical fibers: devices and applications," *Opt. Fiber Technol.* **1**(1), 17–34 (1994).
3. R. M. Measures, "Advances toward fiber optic based smart structures," *Opt. Eng.* **31**(1), 34–47 (1992).
4. Y. Yu et al., "Fiber Bragg grating sensor for simultaneous measurement of displacement and temperature," *Opt. Lett.* **25**(16), 1141–1143 (2000).
5. V. Bhatia et al., "Optical fiber extrinsic fabry-perot interferometric strain sensor for multiple strain state measurements," *Proc. SPIE* **2444**, 115–126 (1995).
6. X. Wang et al., "All-fused-silica miniature optical fiber tip pressure sensor," *Opt. Lett.* **31**(7), 885–887 (2006).
7. E. Cibula et al., "Miniature all-glass robust pressure sensor," *Opt. Express* **17**(7), 5098–5106 (2009).
8. S. J. Mihailov, "Fiber Bragg grating sensors for harsh environments," *Sensors* **12**(2), 1898–1918 (2012).
9. D. W. Kim et al., "Simultaneous measurement of refractive index and temperature based on a reflection mode long-period grating and an intrinsic fabry-perot interferometer sensor," *Opt. Lett.* **30**(22), 3000–3002 (2005).
10. V. E. Zetterlind, III, S. E. Watkins, and M. Spoltman, "Fatigue testing of a composite propeller blade using fiber-optic strain sensors," *IEEE Sens. J.* **3**(4), 393–399 (2003).
11. T. Yoshino et al., "Fiber-optic Fabry-Perot interferometer and its sensor applications," *IEEE J. Quantum Electron.* **18**(10), 1624–1633 (1982).
12. A. D. Kersey, D. A. Jackson, and M. Corke, "A simple fiber Fabry-Perot sensor," *Opt. Commun.* **45**, 71–74 (1983).
13. D. Hogg et al., "Development of a fiber Fabry-Perot strain gauge," *Proc. SPIE* **1588**, 300–307 (1991).
14. W. Zhao et al., "Geometric analysis of optical fiber EFPI sensor performance," *Smart Mater. Struct.* **7**(6), 907–910 (1998).
15. Y. Huang et al., "An extrinsic Fabry–Perot interferometer-based large strain sensor with high resolution," *Meas. Sci. Technol.* **21**(10), 10538 (2010).
16. J. Sirkis et al., "In-line fiber etalon (ILFE) fiber-optic strain sensors," *J. Lightwave Technol.* **13**(7), 1256–1263 (1995).
17. J. Villatoro et al., "Photonic-crystal-fiber-enabled micro-Fabry-Perot interferometer," *Opt. Lett.* **34**(16), 2441–2443 (2009).
18. F. C. Favero et al., "Fabry-Perot interferometers built by photonic crystal fiber pressurization during fusion splicing," *Opt. Lett.* **36**(21), 4191–4193 (2011).
19. F. C. Favero et al., "Spheroidal Fabry-Perot microcavities in optical fibers for high-sensitivity sensing," *Opt. Express* **20**(7), 7112–7118 (2012).
20. Y. J. Rao et al., "Micro Fabry-Perot interferometers in silica fibers machined by femtosecond laser," *Opt. Express* **15**(21), 14123–14128 (2007).
21. E. Cibula et al., "Miniature all-glass robust pressure sensor," *Opt. Express* **17**(7), 5098–5106 (2009).
22. M. Born and E. Wolf, *Principles of Optics*, 6th ed., Pergamon Press, Oxford, UK (1980).
23. A. Kaur et al., "Embeddable fiber optic strain sensor for structural monitoring," *Proc. SPIE* **8692**, 86921W (2013).

Amardeep Kaur is pursuing a PhD in electrical engineering at the Missouri University of Science and Technology (Missouri S&T), Rolla, Missouri. She received her BTech in electronics and communication engineering from Punjab Technical University, India, in 2006 and MS in electrical engineering from Missouri S&T, Rolla in 2008. Her research interests focus on micro/nano optical fiber sensors and structural health monitoring applications. She is a member of SPIE, IEEE, SWE, and IEEE-HKN honor society.

Steve E. Watkins is a professor of electrical and computer engineering and director of the Applied Optics Laboratory at the Missouri University of Science and Technology (formerly the University of Missouri-Rolla), and received a PhD from the University of Texas at Austin in 1989. His memberships include SPIE (senior member), IEEE (senior member), and ASEE. He was an IEEE-USA Congressional Fellow, a visiting physicist at the Phillips Laboratory (USAF), and a visiting scholar at NTT in Japan.

Jie Huang received BS and MS from Tianjin University (2009) and Missouri S&T (2012), respectively. He is currently pursuing a PhD degree at Clemson University. His research interest mainly focuses on the development of photonics and microwave sensors and instrumentations for applications in energy, intelligent infrastructure and biomedical sensing. He was a recipient of the IEEE I&MS graduate fellowship award from 2012 to 2013. He is a member of Omicron Delta Kappa national leadership honor society.

Lei Yuan received his BS in mechanical engineering from Beijing University of Aeronautics and Astronautics, Beijing, China, in 2008. He is currently pursuing a PhD degree in electrical engineering at Clemson University, Clemson, USA. His research interests mainly focus on laser micro/nano fabrication as well as fiber optical sensors and devices for various engineering applications. He is a student member of OSA and SPIE.

Hai Xiao is Samuel Lewis Bell Distinguished Professor of Electrical and Computer Engineering at Clemson University, and received his PhD in electrical engineering from Virginia Tech in 2000. Previously, he was a professor of electrical engineering and director of the Photonics Technology Laboratory at the Missouri S&T. His awards include the Office of Naval Research Young Investigator Program (YIP) Award (2006), the R&D 100 Award (2004), and the Virginia Tech Outstanding Achievement Award (2003).